International Journal of Engineering Science 223 (2026) 104504

Contents lists available at ScienceDirect

International Journal of Engineering Science

journal homepage: www.elsevier.com/locate/ijengsci

Edge-effect and notch-sensitivity in fracture mechanics testing of bending specimens: Ductile-to-brittle-to-ductile double transition by increasing the initial notch depth

Alberto Carpinteri [1], Federico Accornero [2], Bineet Kumar [3,*]

Shantou University, 525063 Shantou, China

ARTICLE INFO

Keywords:
Crack depth
Notch-sensitivity
Ductile-to-brittle-to-ductile double transition
Edge effect

ABSTRACT

The same material may appear to be brittle or ductile depending on the initial relative notch depth and/or the size-scale of the specimen. This study examines the double transition from ductile to brittle and back to ductile for bending-dominated tests, with a special attention to the second transition that appears when the remaining ligament becomes too short for an asymptotic singular stress field to develop. The fracture condition is formulated using published shape functions, and the fracture curves are derived and compared to the single plastic collapse curve for three configurations: pure bending specimens, three-point bend specimens, and compact tension specimens. The notch depth to specimen depth ratio is varied to draw the fracture curves, to identify the transition points, and to relate them to the *brittleness number*. All configurations show the same trends, with a plastic collapse for shallow notches, a brittle window at intermediate notch depths, and a return to plastic collapse for very deep notches. The three-point bend beam returns to ductile behavior for the shortest relative notch depth, representing the most ductile response in the deep notch range. The results confirm that the failure mode depends on material properties, geometrical shape, size-scale of specimen, and initial notch depth. The second transition is a finite-size effect governed by ligament insufficiency, a trend that is analogous to that emerging for extremely small specimen size-scales.

1. Introduction

Fracture mechanics is a cornerstone of mechanical engineering, providing a clear insight into failure mechanisms and size-scale transitions from ductile to brittle responses. The same material may appear to be brittle or ductile depending on the size-scale of the specimen and/or the initial relative notch depth. Objective of this study is the double transition from ductile to brittle and back to ductile by increasing the initial notch depth, with a special attention to the second transition that appears when the remaining ligament becomes too short for an asymptotic singular stress field to develop.

Scaling, as the competition between two different structural collapses governed by generalized forces with different physical

* Corresponding author.
E-mail address: bineetkumar@stu.edu.cn (B. Kumar).
[1] Chair Professor
[2] Associate Professor
[3] Post-doctoral Researcher

https://doi.org/10.1016/j.ijengsci.2026.104504
Received 9 December 2025; Received in revised form 15 February 2026; Accepted 15 February 2026
Available online 21 February 2026

Nomenclature

s	Brittleness number
a_0	Initial notch length
b	Depth of the beam specimen
K_{IC}	Fracture toughness
l	Span length of the beam specimen
σ_P	Yield strength

dimensions (plastic collapse and brittle fracture), should be clearly distinguished from the well-known t*hickness* (or *constraint*) effect, which considers the extension of the crack tip plastic zone as varying through the specimen thickness, keeping the remaining planar dimensions constant. The latter derives from the transition between plane-stress and plane-strain conditions by increasing the plate thickness. In metals, the two effects are both present and interacting, whereas in concrete-like materials only the planar scaling effect is present without any possibility of superposing and confusing the two effects (thanks to the low Poisson ratio).

In addition, the two effects show the same trend towards brittleness by increasing either the planar size-scale or the plate thickness, although they are independent and orthogonal. Even if it is not the scope of the present paper, it should not be difficult to generalise the present results to the interactions between the two effects by simply considering the apparent fracture toughness of the material as a function of the plate thickness.

The previous arguments represent the reason why scale effects were firstly studied and solved in the scientific community of concrete materials and structures. Two intrinsic characteristics of the material (strength and toughness) plus a geometrical characteristic of the structure represent the minimum information to predict the structural response. As in structures prevalently subjected to compression forces a transition occurs from plastic collapse (in compression) to buckling by increasing their slenderness, so in structures subjected to tensile forces a transition occurs from plastic collapse to brittle fracture by increasing their size-scale.

Two well-known extreme cases, over seven orders of magnitude in length-scale, are represented by Liberty ships and glass filaments. During the Second World War (Kirk, Dodds and Jr, 1993), ships suddenly split into two parts, showing extremely brittle fractures without any slightest fore-warning evidence. At that time, astonishment in technicians and researchers was due to the contrast between the extreme brittleness of the failures and the considerable ductility shown in the laboratory by specimens of the same steel.

On the other hand, considering a microscopic filament of glass used for fiber reinforcement, it has been proven to bear large strains and stresses up to two orders of magnitude greater than the tensile limits of the glass itself, when measured at the laboratory scale with specimens of normal dimensions. These two examples remark how both strength and ductility appear to be functions of the structural scale.

In the framework of solid and fluid mechanics, the explanations to scale dependent transitions, such as ductile-to-brittle and laminar-to-turbulent, are based on dimensional analysis and the Π Buckingham's theorem.

Erdogan and Sih (Erdogan and Sih) provided the first systematic analysis of the edge effect. They compared plane-stress and plane-strain conditions but did not address the potential interaction between brittle crack propagation and plastic collapse. In the same years, Tada,Paris, and Irwin (Tada et al., 1973) compiled a comprehensive set of analytical solutions for stress-intensity factors in cracked beams and plates. These closed-form or series-expansion expressions became standard references in stress and fracture analysis and still are widely used in the engineering practice. The role of edge effects was explored further by Murakami (Murakami), who carried out extensive fatigue tests on edge-cracked specimens.

Nakamura and Parks (Nakamura and Parks, 1989) used three-dimensional finite element analysis to track how the stress field varies along the crack front as it approaches a free edge under different loading conditions. Rice (Rice) showed how plastic deformation at a crack tip depends on constraint. On the other hand, his formulation did not address the potential interaction between distinct failure mechanisms acting through generalized forces of different physical dimensions, namely, the plastic-flow collapse at the ligament and the brittle crack propagation.

Thin sections lower constraint and allow plasticity to spread (Kaplan, 1961, Nelson et al., 1972). Hutchinson (Hutchinson, 1976) examined how constraint affects fracture toughness in plates and showed that the transition to brittleness becomes more pronounced when plastic flow is limited by constraint.

The initial notch depth also plays a central role in the ductile-to-brittle transition. Gao and Ritchie (Gao and Ritchie, 1989) showed that deep notches raise stress triaxiality, which suppresses plastic flow and promotes brittle responses. Neuber (Neuber and Kerbspannungslehre) developed early notch-analysis models demonstrating that sharp notches amplify local stress and increase susceptibility to brittle failure. McClintock and Argon (McClintock and Argon) linked plasticity at the notch root with the initiation of brittle fracture and reported that materials with low strain-hardening capacity can fail in a brittle manner at smaller notch depths. Ritchie and Knott (Ritchie and Knott, 1973) confirmed experimentally that brittle initiation occurs at a critical notch depth, beyond which plastic deformation is no longer sufficient to prevent sudden fracture. Hahn and Rosenfield (Hahn and Rosenfield, 1965) studied high-strength steels and found that the transition temperature shifts to higher values as notch acuity increases. Kirk and Dodds (Kirk, Dodds and Jr, 1993) used finite-element analyses of pre-cracked specimens to show that the higher constraint associated to deep notches reduces the effectiveness of plastic toughening mechanisms, making brittle fracture more likely.

All previous references show how a clear distinction between the two size transitions has never been made so far. The well-known

thickness or constraint effect experimentally often interacts with the planar size-scale effect. They are different in nature, the former representing a transition between plane-stress and plane-strain conditions, whereas the latter represents a planar scale transition between plastic-flow collapse and brittle crack propagation (Carpinteri, 1982, Carpinteri, 2021, Sneha and Ray, 2025).

As regards the experimental results, especially related to the second brittle-to-ductile transition, we can say that very few data are available, the tests very unfrequently contemplating deep initial cracks. Nevertheless, an interesting confirmation by published results of the first author will be provided. As regards the well-known Failure Analysis Diagram (FAD), it is based on the same strategy proposed in the present contribution: that of separately considering brittle crack propagation and plastic collapse at the ligament as potential failure modes. On the other hand, FAD is developed in a totally different way (using the debated concept of J-integral), without considering the scale effects explicitly, as proposed herein and in different preceding papers of the first author.

2. Ductile-to-brittle-to-ductile double transition

Irwin (Irwin) proposed a characteristic flaw size a_0 (semi-length) for ductile materials. When the crack or notch is shorter than $2a_0$, plastic deformation spreads ahead of the tip and the nominal response is governed by general yielding. When the flaw size exceeds $2a_0$, the stress-singularity dominates and the stress-intensity factor reaches the material's fracture toughness before plastic flow wide-spreads, so that brittle behavior manifests. This threshold follows from equating LEFM condition and generalized yielding condition:

$$a_0 = \frac{1}{\pi}\frac{K_{IC}^2}{\sigma_P^2} \tag{1}$$

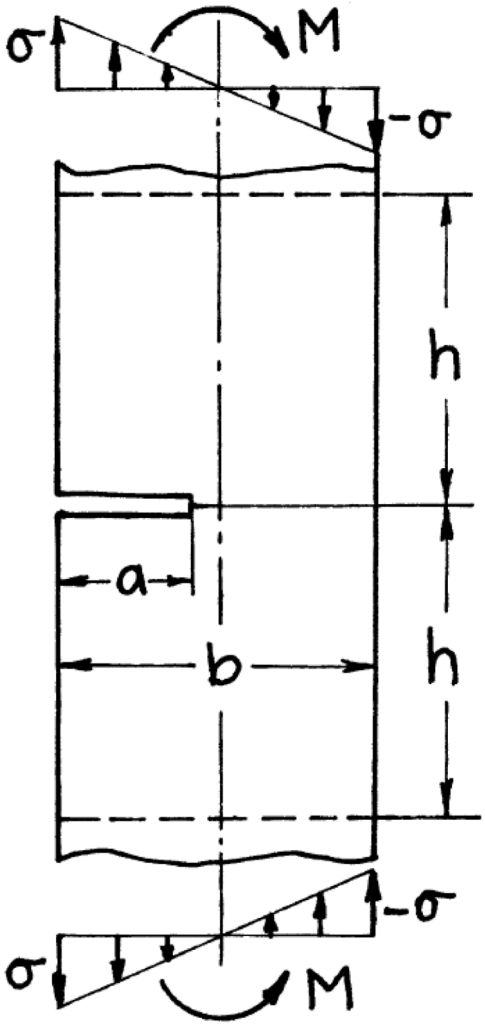

Fig. 1. Pure-bending test specimen.

where K_{IC} represents the fracture toughness, and σ_P the yield strength of the material. The two distinct and co-existing failure criteria for an infinite plate are:

$$\sigma = \frac{1}{\sqrt{\pi}} \frac{K_{IC}}{\sqrt{a}}, \text{ for } a > a_0 \tag{2}$$

$$\sigma = \sigma_P, \text{ for } a < a_0 \tag{3}$$

The foregoing discussion shows that the ductile-to-brittle transition evolves by increasing the notch depth. Carpinteri (Carpinteri, 1982, Carpinteri, 2021) extended this argument to finite geometries and introduced the *Brittleness Number s* to represent the combined effect of material properties and planar size-scale of the specimen (plane-stress condition):

$$s = \frac{K_{IC}}{\sigma_P \sqrt{b}} \tag{4}$$

where b is the depth or width of the specimen. The stress-intensity factor, when the plate is not infinite, is expressed through a shape-function factor that takes into account the finite geometry of the specimen (Sih):

$$K_I = \sigma \sqrt{\pi a}\, F(a/b) \tag{5}$$

where $F(a/b)$ is the *shape-function* depending on the specimen geometry and on the relative notch depth a/b (Shah and McGarry, 1971, Tada et al., 1973). These studies show that the notch-sensitivity is a key aspect.

As a/b increases, the increment in $F(a/b)$ creates a notch depth interval where brittle crack extension is favored, although for very deep notches the remaining ligament may no longer sustain an asymptotic singular stress field and plastic collapse reappears. Onset and extension of this brittle-to-ductile transition are therefore geometry-dependent (Carpinteri, 1982, Carpinteri, 2021). In the present study, this transition is examined for different bending geometries using available shape-functions to express the fracture condition and to identify the onset of the brittle-to-ductile return.

The ductile–to-brittle–to-ductile double transition is a key aspect in fracture mechanics. Understanding this transition clarifies whether failure will occur abruptly with little warning or after visible plastic deformation, which has direct implications to safety and design.

The geometries examined are the pure-bending (PB) test specimen, the three-point bend (TPB)test specimen, and the compact tension (CT) test specimen. For each case, the fracture curves are derived using a linear elastic fracture mechanics (LEFM) approach based on the available shape-functions $F(a/b)$. Specimen size and notch depth are varied to draw the fracture curves and to compare them to the single plastic-collapse limit curve. On this basis, the brittle-to-ductile transition crack depth is identified as a function of the brittleness number s.

3. Pure bending test specimen

A pure bending specimen of depth b, infinite length, and with an edge crack of depth a is shown in Fig. 1. It is subjected to the bending moment M. It is interesting to analyze its critical bending moment as a function of the crack depth to specimen depth ratio and varying the parameter s. In the present case, the induced bending stress σ is expressed as:

$$\sigma = \frac{6M}{b^2 t} \tag{6}$$

whereas the critical bending moment due to the achievement of fracture toughness is:

$$\frac{M_{CR}}{\sigma_P b^2 t} = \frac{s}{6F(a/b)} \tag{7}$$

The two failure criteria, for ultimate strength and for plastic collapse (plastic hinge formation at the ligament) are expressed as follows:

Ultimate strength limit

$$\frac{M_{CR}}{\sigma_P b^2 t} = \frac{1}{6}(1 - a/b)^2 \tag{8}$$

Plastic collapse limit

$$\frac{M_{CR}}{\sigma_P b^2 t} = \frac{1}{4}(1 - a/b)^2 \tag{9}$$

The available shape functions, in the case of pure bending, are applicable in the range $0 < a/b \leq 0.99$:
Tada (Tada et al., 1973)

$$F(a/b) = \sqrt{\frac{2b}{\pi a}\tan\frac{\pi a}{2b}}\left[\frac{0.923 + 0.199\left(1 - \sin\frac{\pi a}{2b}\right)^4}{\cos\frac{\pi a}{2b}}\right] \tag{10}$$

Wilson (Tada et al., 1973, Wilson, 1970)

$$F(a/b) = 2(a/b)^{1/2} - 2.435(a/b)3\Big/2 + 10.19(a/b)^{5/2} - 7.912(a/b)^{7/2} + 27.03(a/b)^{13/2} - 16.51(a/b)^{15/2} \tag{11}$$

Figs. 2 and 3 show the variation in the normalized critical fracture moment with a/b. The families of curves are drawn by utilizing Eq. 7 for different values of s. The dashed thick black line represents the ultimate strength limit (see Eq. 8), whereas Eq. 9 is utilized to represent the plastic collapse limit, see the continuous thick black line.

As s increases, the brittle window contracts. At $s \approx 0.78$, the fracture curve becomes tangent to the plastic-collapse curve (Fig. 4). Predictions obtained using the different shape functions essentially are indistinguishable.

4. Three-point bend test specimen

A three-point bend test specimen of depth b, span l, thickness t, with an edge crack of depth a and the centrally applied load P, is shown in Fig. 5. Its critical bending moment is a function of the crack depth to specimen depth ratio and varying with the parameter s. In the present case, the induced bending stress σ is expressed as in Eq. 6 with $M = Pl/4$, whereas the critical bending moment due to the achievement of fracture toughness is:

$$\frac{P_{CR}l}{\sigma_P b^2 t} = \frac{2}{3}\frac{s}{F(a/b)\sqrt{\frac{\pi a}{b}}} \tag{12}$$

Below are the available shape-functions in the case of three-point bend beam for span to depth ratio of 4, and applicable in the range $0 < a/b \leq 0.99$.

Srawley (Tada et al., 1973)

$$F(a/b) = \frac{1}{\sqrt{\pi}}\frac{1.99 - a\Big/b(1-a/b)\left(2.15 - 3.93a\Big/b + 2.7(a/b)^2\right)}{(1+2a/b)(1-a/b)^{3/2}} \tag{13}$$

ASTM (E-399) (Srawley, 1976)

$$F(a/b) = 2.9(a/b)^{1/2} - 4.6(a/b)^{3/2} + 21.8(a/b)^{5/2} - 37.6(a/b)^{7/2} + 38.7(a/b)^{9/2} \tag{14}$$

The two failure criteria in the case of three-point bend beam are:

Ultimate strength limit

$$\frac{P_{CR}l}{\sigma_P b^2 t} = \frac{2}{3}(1 - a/b)^2 \tag{15}$$

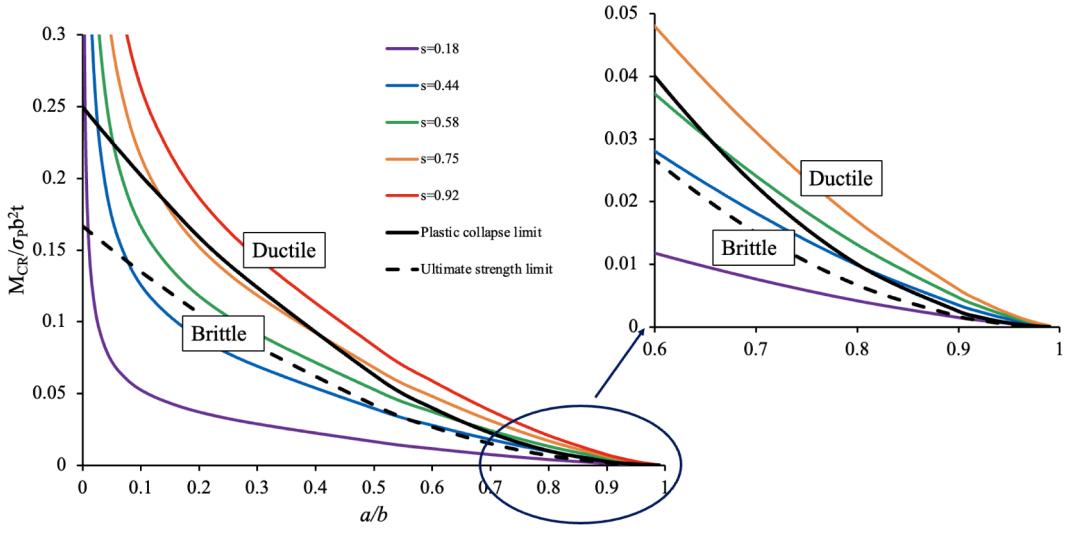

Fig. 2. Pure bending test specimen: Nondimensional crack extension moment as a function of the relative crack depth and by varying the brittleness number s (Tada).

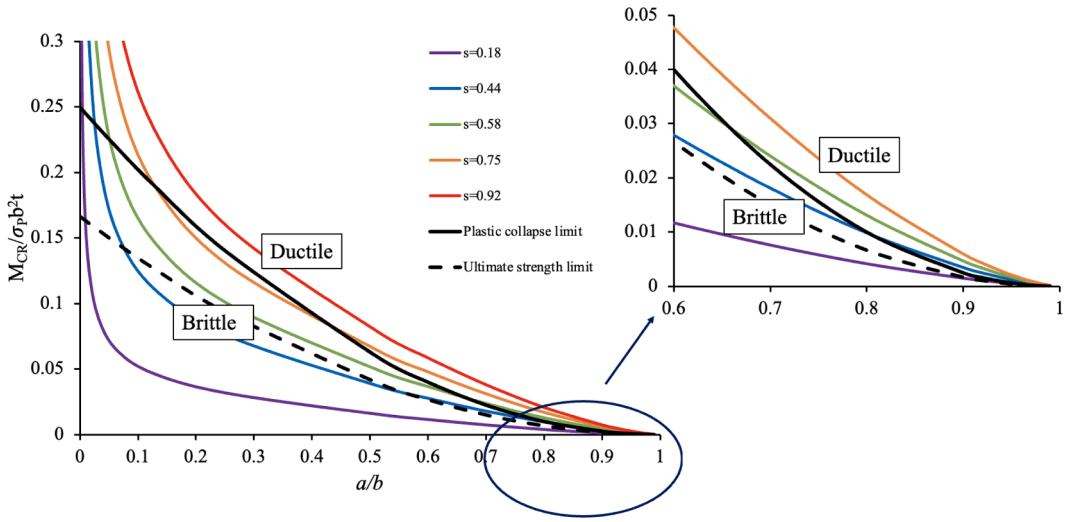

Fig. 3. Pure bending test specimen: Nondimensional crack extension moment as a function of the relative crack depth and by varying the brittleness number *s* ((Wilson).

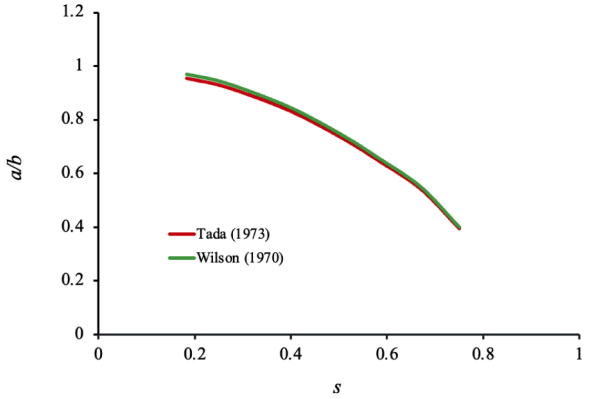

Fig. 4. Pure bending test specimen: Brittle-to-ductile transition value of the relative crack depth as a function of the brittleness number *s* and for different shape functions.

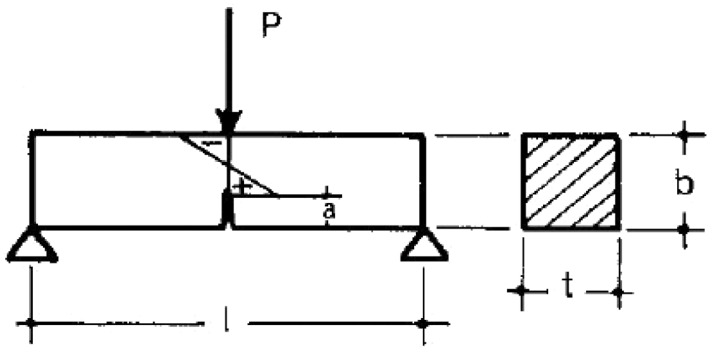

Fig. 5. Three-point bend test specimen.

Plastic collapse limit

$$\frac{P_{CR}l}{\sigma_P b^2 t} = (1 - a/b)^2 \tag{16}$$

Figs. 6 and 7 show the ductile–to-brittle–to-ductile double transition for different curves obtained by varying s. The fracture curve becomes tangent to the plastic-collapse limit for $s \approx 0.75$, which is comparable to the value of the pure-bending specimen. For brittleness numbers higher than such limit value, any transition disappears and only the plastic collapse remains as potential collapse mechanism

Fig. 8 compares the shape functions used to draw the diagrams. For large a/b, the predictions diverge, whereas differences appear for small a/b.

5. Compact tension test specimen

Fig. 9 shows the compact tension test specimen under the applied load P. Here, the stress-intensity factor K_I can be calculated by using Eqs. 18, 19, and the shape-function expressed by Eq. 21. The failure load can be derived from Eq. 20, through Eqs. 4, 18, and 19:

$$K_I = \sigma\sqrt{b-a}F(a/b) \tag{17}$$

$$\sigma = \frac{2P(2b+a)}{t(b-a)^2} \tag{18}$$

$$\frac{P_{CR}}{\sigma_P bt} = \frac{s}{2F(a/b)\sqrt{b}}\frac{(b-a)^{3/2}}{2b+a} \tag{19}$$

Below is the available shape function for compact tension test specimen ($h/b = 0.6$; $d/b = 0.27$), applicable in the range of $0.2 \leq a/b \leq 0.99$:

Srawley (Srawley, 1976, Tada etal., 1973)

$$F(a/b) = 0.443 + 2.32(a/b) - 6.66(a/b)^2 + 7.36(a/b)^3 - 2.8(a/b)^4 \tag{20}$$

Similarly to the previous cases, the two failure criteria are:

Ultimate strength limit

$$\frac{P_{CR}}{\sigma_P bt} = \frac{(1-a/b)^2}{(2a/b+4)} \tag{21}$$

Plastic collapse limit

$$\frac{P_{CR}}{\sigma_P bt} = \frac{(1-a/b)^2}{(3+a/b)} \tag{22}$$

Figure 10 shows the critical load as a function of a/b and by varying s. The compact-tension specimen exhibits the same ductile–to-

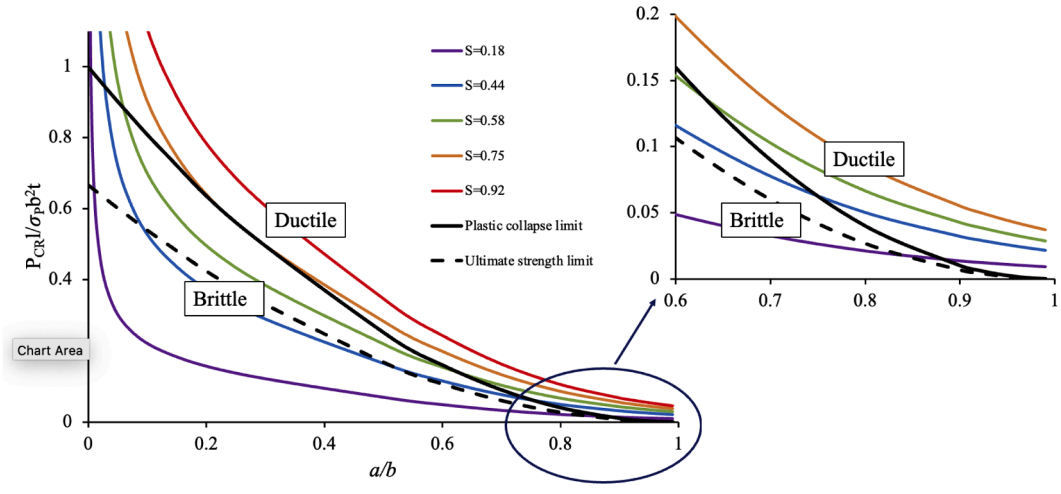

Fig. 6. Three-point bend test specimen: Nondimensional force of crack extension as a function of the relative crack depth and by varying the brittleness number s (ASTM E 399).

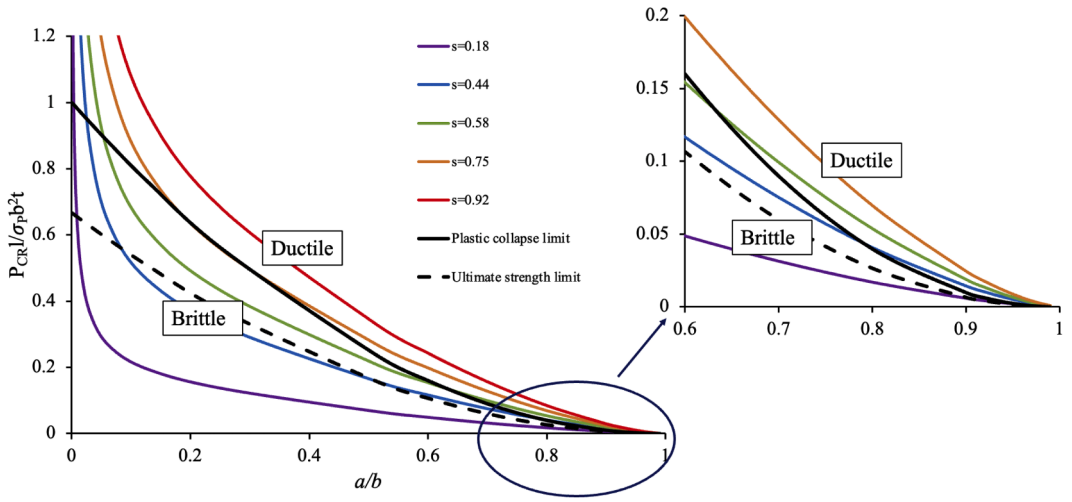

Fig. 7. Three-point bend test specimen: Nondimensional force of crack extension as a function of the relative crack depth and by varying the brittleness number *s* (Srawley).

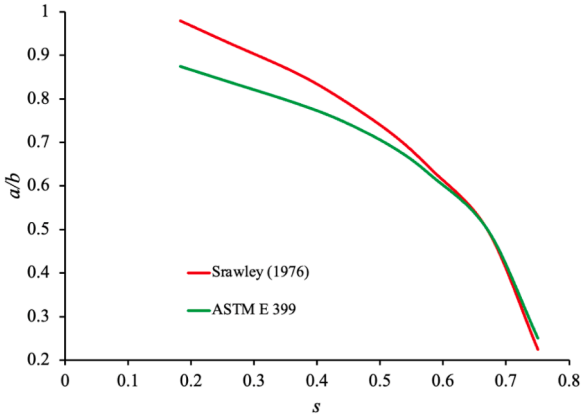

Fig. 8. Three point bend test specimen: Brittle-to-ductile transition value of the relative crack depth as a function of brittleness number *s* and for different shape functions.

brittle–to-ductile double transition as the other cases: at small a/b the plastic limit of the ligament governs; at intermediate a/b a brittle window opens; and at sufficiently deep notches the response returns to plastic collapse. For this geometry, the brittle-to-ductile return begins at about $a/b \approx 0.45$ (Fig. 11), as well as the fracture curve becomes tangent to the plastic-collapse curve at $s \approx 0.85$. Beyond this tangency, the fracture criterion no longer governs and the response is controlled by plastic collapse. The trend is consistent with the pure-bending and three-point bending results (Fig. 12).

6. Discussion and conclusions

This study demonstrates that the failure mode is governed not only by the intrinsic material properties, but also by the specimen dimensions and the initial relative notch depth. In particular, a second transition of the fracture advancement towards the opposite edge or boundary is identified, which is rarely discussed, whereas the first transition from the original edge has been well-known since the early developments of fracture mechanics. The first ductile-to-brittle transition also occurs in plates that can be treated as infinite, whereas the second brittle-to-ductile transition appears only in finite geometries, where the remaining ligament is too short for the stress-singularity field to fully develop.

The paper intends to represent a theoretical contribution, since the experimental cases have been already reported in previous papers by the first author. Unfortunately, the experiments on notch-sensitivity for deep initial notches are nearly absent in the scientific literature as in his previous experimental publications, except for one case regarding high-strength concrete beams, where the plastic collapse at the ligament is replaced by an ultimate-strength collapse, confirming the relevant conclusions of this paper.

In (Biolzi et al., 1989), a total of 18 beam specimens of high-strength concrete were tested in three-point bending, all of them presenting the same dimensions (depth = 100 mm, length = 400 mm, thickness = 50 mm) and different initial notch depths: 5, 10, 20,

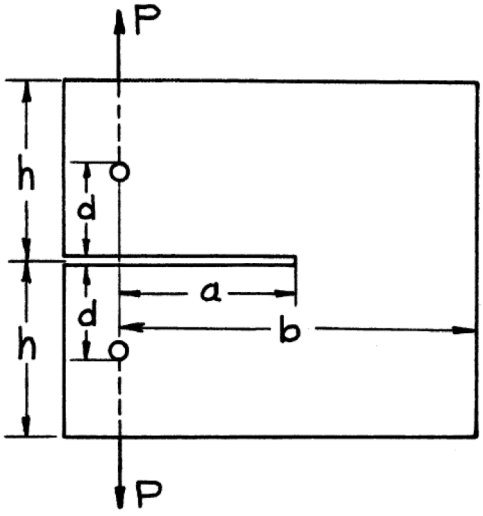

Fig. 9. Compact tension test specimen.

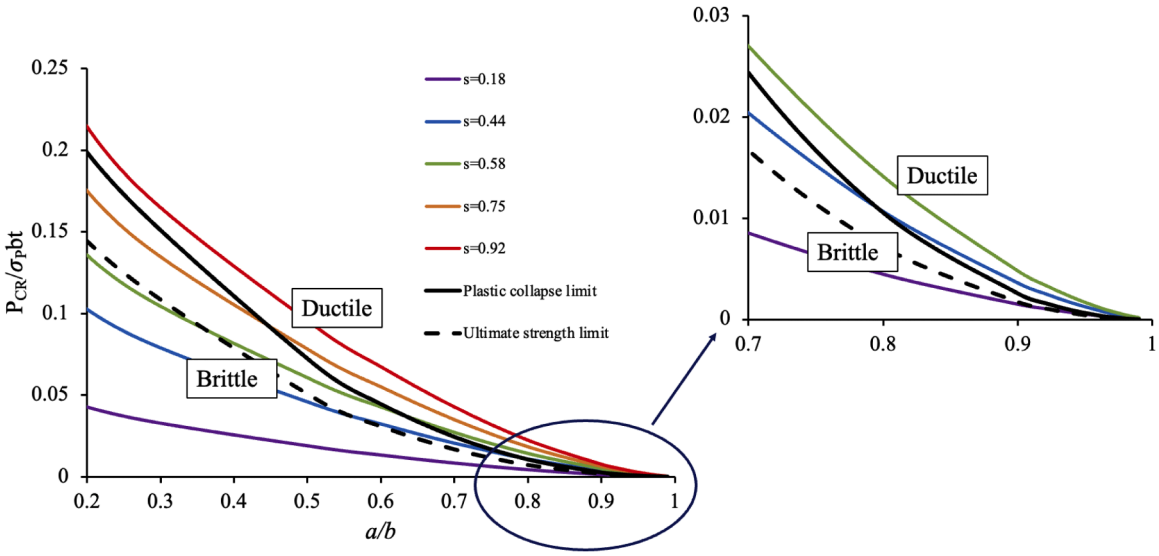

Fig. 10. Compat tension test specimen: Nondimensional crack extension force as a function of the relative crack depth and by varying the brittleness number *s* (Srawley).

30, 40, 50, 60, 70, 80 mm, two identical specimens for each initial notch depth. In Fig. 13, the apparent values of fracture toughness are represented, based on the experimental values of the peak load. The central values between 10 and 40 mm are aligned along a horizontal plateau and represent a true LEFM crack propagation, whereas the values at 5 and between 50 and 80 mm belong to the two external branches and represent an ultimate-strength failure anticipating the potential LEFM crack propagation.

The analytical curves introduced in the paper are not abstract, they have to be interpreted on the basis of Buckingham's Theorem for physical similitude and scale modelling that has never been applied in Material Strength. Nobody has taken care of the double transition so far, except the first author (Carpinteri, 1982, Carpinteri, 2021). The experimental implications of the theoretical results are explained in the present paper in detail.

It is opportune to recall FAD because it adopts the same strategy and philosophy of considering two different failure modes separately. On the other hand, explicit assumption in the present paper is that of emphasizing the different physical dimensions of strength and toughness and introducing the *Brittleness Number*, which results to be a simple, rational, and rigorous approach.

Also the interaction between planar scale effects and thickness effects must be emphasized.

Scale effects, as the competition between two different structural collapses governed by generalized forces with different physical dimensions (plastic collapse and brittle fracture), should be clearly distinguished from the well-known *thickness* (or *constraint*) *effects*, which consider the extension of the crack tip plastic zone as varying through the specimen thickness, keeping the remaining planar

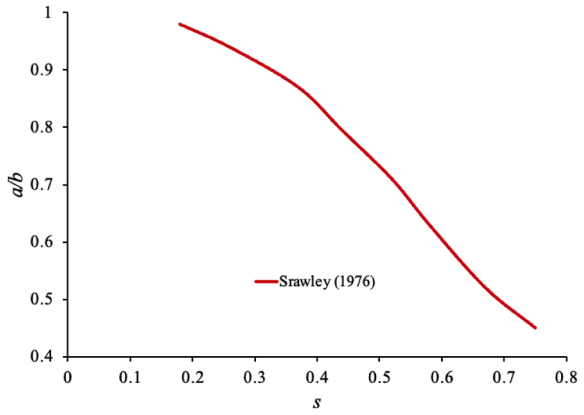

Fig. 11. Compact tension test specimen: Brittle-to-ductile transition value of the relative crack depth as a function of the brittleness number *s*.

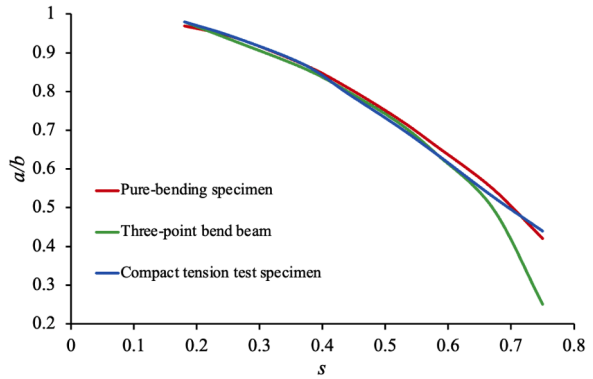

Fig. 12. Brittle-to-ductile transition value of the relative crack depth as a function of the brittleness number *s*. Comparison between different specimen geometries, considering the shape function by Wilson for pure bending, and the shape functions by Srawley for three-point bending and compact tension.

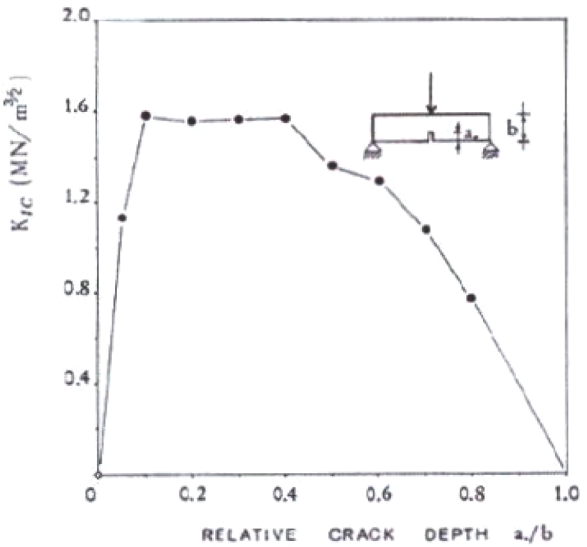

Fig. 13. Apparent fracture toughness values, according to LEFM and calculated on the basis of experimental peak loads, versus relative initial notch depth. The central plateau represents true LEFM crack propagations, whereas the lateral branches correspond to ultimate-strength collapse.

dimensions constant. The latter derives from the transition between plane-stress and plane-strain conditions by increasing the plate thickness. In metals, the two effects are both present and interacting, whereas in concrete-like materials only the planar scaling effect is present without any possibility of superposing and confusing the two effects (thanks to the low Poisson ratio).

In addition, the two effects show the same trend towards brittleness by increasing either the planar size-scale or the plate thickness, although they are independent and orthogonal. Even if it is not the scope of the present paper, it should not be difficult to generalise the present results to the interactions between the two effects by simply considering the apparent fracture toughness of the material as a function of the plate thickness.

The previous arguments represent the reason why scale effects were firstly studied and solved in the scientific community of concrete materials and structures. Two intrinsic characteristics of the material (strength and toughness) plus a geometrical characteristic of the structure represent the minimum information to predict the structural response. As in structures prevalently subjected to compression forces a transition occurs from plastic collapse (in compression) to buckling by increasing their slenderness, so in structures prevalently subjected to tensile forces a transition occurs from plastic collapse to brittle fracture by increasing their size-scale.

In the framework of solid and fluid mechanics, the explanations to scale dependent transitions, such as ductile-to-brittle and laminar-to-turbulent, are based on dimensional analysis and the Π Buckingham's Theorem

Tending to zero for the ligament (or to unity for the relative crack depth) is equivalent to tending to zero for the depth of an initially uncracked beam. In both cases, a perfectly-plastic collapse asymptotically prevails.

CRediT authorship contribution statement

Alberto Carpinteri: Writing – review & editing, Visualization, Supervision, Methodology, Investigation, Conceptualization. **Federico Accornero:** Supervision, Methodology, Data curation, Conceptualization. **Bineet Kumar:** Writing – review & editing, Writing – original draft, Methodology, Investigation, Formal analysis, Data curation, Conceptualization.

Declaration of competing interest

The authors declare that they have no known competing financial interests or personal relationships that could have appeared to influence the work reported in this paper.

Data availability

Data will be made available on request.

References

Biolzi, L., Cangiano, S., Tognon, G., & Carpinteri, A. (1989). Snap-back softening instability in high strength concrete bems. *Materials and Structures, 22*, 429–436.

Carpinteri, A. (1982). Notch sensitivity in fracture testing of aggregative materials. *Engineering Fracture Mechanics, 16*(4), 467–481.

Carpinteri, A. (2021). *Fracture and Complexity*. Heidelberg: Springer Nature.

F. Erdogan, G. Sih, On the crack extension in plates under plane loading and transverse shear.

Gao, H., & Ritchie, R. O. (1989). Brittle fracture in ductile materials. *Annual Review of Materials Science, 29*(1), 173–208.

Hahn, G. T., & Rosenfield, A. R. (1965). Local yielding and extension of a crack under plane stress. *Acta Metallurgica, 13*(3), 293–306.

Hutchinson, J. W. (1976). Plastic flow and fracture in solids. *Advances in Applied Mechanics, 16*, 67–140.

G. R. Irwin, Analysis of stresses and strains near the end of a crack traversing a plate.

Kaplan, M. (1961). Crack propagation and the fracture of concrete. *Journal Proceedings, 58*, 591–610.

Kirk, M. T., Dodds, R. H., & Jr, J. (1993). CTOD estimation equations for shallow cracks in single edge notch bend specimens. *Journal of Testing and Evaluation, 21*(4), 228–238.

F. A. McClintock, A. S. Argon, Mechanical behaviour of materials.

Y. Murakami, Stress intensity factors handbook, Soc. Mater. Sci., Japan.

Nakamura, T., & Parks, D. M. (1989). Anti-symmetric stress intensity factors for interface cracks. *International Journal of Fracture, 40*(1), 103–121.

Nelson, F., Schilling, P., & Kaufman, J. (1972). The effect of specimen size on the results of plane-strain fracture-toughness tests. *Engineering Fracture Mechanics, 4*(1), 33–50.

H. Neuber, S. Kerbspannungslehre, Translation theory of notch stresses, US Office of Technical Services, Washington, DC.

J. R. Rice, A path independent integral and the approximate analysis of strain concentration by notches and cracks.

Ritchie, R., & Knott, J. (1973). Mechanisms of fatigue crack growth in low alloy steel. *Acta Metallurgica, 21*(5), 639–648.

Shah, S. P., & McGarry, F. J. (1971). Griffith fracture criterion and concrete. *Journal of the Engineering Mechanics Division, 97*(6), 1663–1676.

G. Sih, Handbook of stress-intensity factors for researchers and engineers, Institute of Fracture and Solid Mechanics, Lehigh University, Bethlehem, PA.

Sneha, B. Kumar, & Ray, S. (2025). Notch sensitivity on post-cracking behaviour of ultra-high-performance fibre-reinforced concrete. *Theoretical and Applied Fracture Mechanics, 138*, Article 104925.

Srawley, J. E. (1976). Wide range stress intensity factor expressions for ASTM E-399 standard fracture toughness specimens. In *Conf. of Am. Soc. for Testing and Mater.* Committee E-24.

Tada, H., Paris, P. C., & Irwin, G. R. (1973). *The stress analysis of cracks, Handbook, 34*. Del Research Corporation.

Wilson, W. (1970). Stress intensity factors for deep cracks in bending and compact tension specimens. *Engineering Fracture Mechanics, 2*(2), 168–171.